Surface core level shifts of clean and oxygen covered Ir(111)

2009 New J. Phys. 11 063002

(http://iopscience.iop.org/1367-2630/11/6/063002)

New Journal of Physics
The open-access journal for physics

Surface core level shifts of clean and oxygen covered Ir(111)

M Bianchi[1], D Cassese[1], A Cavallin[1], R Comin[1], F Orlando[1], L Postregna[1], E Golfetto[2,3], S Lizzit[4] and A Baraldi[2,3,5]

[1] Università degli Studi di Trieste, Via A Valerio 2, 34127, Trieste, Italy
[2] Dipartimento di Fisica e CENMAT, Università degli Studi di Trieste, Via A Valerio 2, 34127, Trieste, Italy
[3] Laboratorio Nazionale TASC INFM-CNR, AREA Science Park, 34012 Trieste, Italy
[4] Sincrotrone Trieste S.C.p.A., S.S. 14 Km 163.5, 34012 Trieste, Italy
E-mail: alessandro.baraldi@elettra.trieste.it

New Journal of Physics **11** (2009) 063002 (18pp)
Received 17 February 2009
Published 3 June 2009
Online at http://www.njp.org/
doi:10.1088/1367-2630/11/6/063002

Abstract. We present the results of high resolution core level photoelectron spectroscopy employed to investigate the electronic structure of clean and oxygen covered Ir(111) surface. Ir $4f_{7/2}$ core level spectra are shown to be very sensitive to the local atomic environment. For the clean surface we detected two distinct components shifted by 550 meV, originated by surface and bulk atoms. The larger Gaussian width of the bulk component is explained as due to experimentally unresolved subsurface components. In order to determine the relevance of the phonon contribution we examined the thermal behaviour of the core level lineshape using the Hedin–Rosengren theory. From the phonon-induced spectral broadening we found the Debye temperature of bulk and surface atoms to be 298 and 181 K, respectively, which confirms the softening of the vibrational modes at the surface. Oxygen adsorption leads to the appearance of new surface core level components at −200 meV and +230 meV, which are interpreted as due to first-layer Ir atoms differently coordinated with oxygen. The coverage dependence of these components demonstrates that the oxygen saturation corresponds to 0.38 ML, in good agreement with recent density functional theory calculations.

[5] Author to whom any correspondence should be addressed.

Among the 5d transition metals, Ir exhibits distinctive physical and chemical properties which are largely employed in industrial applications, especially in heterogeneous catalysis, where it is used to improve the selectivity towards N_2 rather than NO_x production during ammonia oxidation [1] and for the high efficiency in C–H bond breaking [2]. Indeed the (111) surface of Ir was recently used to grow highly ordered graphene layers using ethylene [3]. Therefore, the study of the electronic properties of Ir surface atoms and their modification upon annealing and interaction with adsorbed species is of crucial importance for an accurate and quantitative understanding of the aforementioned processes.

High resolution x-ray photoelectron spectroscopy (HR-XPS) has been exploited since the 1980s to study the outermost layers of a solid sample, thanks to the high sensitivity to the local chemical environment of surface atoms [4]. Because of their localized nature, core electrons are influenced by the electronic charge redistribution resulting from the breaking of the translational symmetry and the reduced coordination at the surface. This results in a difference between the core-level binding energies (BEs) of surface and bulk atoms, called surface core-level shift (SCLS) [5]–[7]. HR-XPS has been exploited to measure the SCLSs of clean and adsorbate covered surfaces and on a large variety of 5d transition metal surfaces, like Ta [8, 9], W [10]–[12], and Pt [13, 14].

In their pioneering work Van der Veen *et al* [15] investigated the $4f_{7/2}$ surface core-level BEs and intensities of (001) and (111) Ir surfaces, showing for the first time that these quantities give direct access to surface structural information. The $4f_{7/2}$ core level was decomposed into bulk and surface contributions with SCLS of -0.50 eV. More recently Gladys *et al* [16] employed XPS using synchrotron radiation to investigate 4f core-level features of differently prepared Ir stepped surfaces. For clean planar Ir(210) three surface Ir $4f_{7/2}$ features were observed with core-level shifts of -765, -529 and -281 meV with respect to the bulk, associated with first-, second- and third-layer atoms, respectively. These results are consistent with the theoretical prediction based on the equivalent core approximation by Johansson and Mårtensson [17], which suggests that all surface features should experience BE shifts to smaller values than the bulk component.

In the present work we investigate the Ir $4f_{7/2}$ SCLS, focussing on the following aspects: (i) the lineshape at low temperature, (ii) the thermally induced broadening and BE shifts and (iii) the oxygen induced SCLS. We find the SCLS of the clean Ir(111) surface to be -550 meV, larger than the previously measured value. The large Gaussian width of the bulk component, which cannot be explained neither in terms of inhomogeneous broadening nor in terms of enhanced phonon contribution, is most probably due to the presence in the bulk peak region of experimentally unresolved subsurface layer components. The large difference of the temperature dependence of surface and bulk Gaussian widths is described as due to the enhanced vibrations at the surface and a lower surface Debye temperature ($T = 181$ K) with respect to the bulk value ($T = 298$ K), in agreement with previous low energy electron diffraction (LEED) results [18]. Finally, oxygen adsorption at room temperature results in the occupation of a single adsorption site [19, 20], while the saturation coverage, as estimated by the changes of the Ir $4f_{7/2}$ core level, is found to be 0.38 ± 0.04 ML. This result reconciles the differences between experimental findings [21, 22] and recent *ab initio* theoretical calculations [23] which suggest that in the narrow range of the oxygen chemical potential achievable in ultra high vacuum (UHV) conditions, the $p(2 \times 1)$ structure at 0.5 ML is unstable.

The photoemission experiments have been performed at the SuperESCA beamline of ELETTRA, the synchrotron facility in Trieste, Italy [24]. The Ir(111) crystal was cleaned

with Ar^+ sputtering ($T = 300$ K, $E = 3$ keV) and annealing cycles ($T = 1320$ K) followed by oxygen treatments at 900–1200 K ($p = 1 \times 10^{-7}$ mbar). At the end of these cycles, hydrogen reduction was used to remove the residual oxygen. The whole procedure was repeated until the C1s and O1s regions of the core-level spectra did not show any trace of contaminants and a sharp (1×1) LEED pattern was observed. During the measurements the base pressure in the UHV experimental chamber was kept at 1×10^{-10} mbar (residual gases consisting mainly of hydrogen and carbon monoxide). Nevertheless, in order to keep the surface contamination at a very low level (below 0.5% ML), the sample was annealed to 670 K at intervals of about 10 min. This results in desorption of the main contaminants, such as hydrogen, carbon monoxide and water. In fact, it is well known that even very small amounts of adsorbed impurities can modify the shape of the core-level spectra, as they generate new surface core level-shifted components at different BEs with respect to the clean surface.

The sample was cooled by liquid nitrogen and heated by electron bombardment from hot tungsten filaments mounted behind it. High energy resolution Ir $4f_{7/2}$ core-level spectra were collected using photon energies from 140 to 200 eV with an overall energy resolution of about 40 meV, as determined by measuring the width of the Fermi level of a Ag polycrystal. In order to minimize the effect of phonon broadening, the sample was mounted on a liquid helium cryostat, which permits cooling down to 80 K when using liquid nitrogen. Temperature dependent core level spectra were measured only during cooling cycles in order to avoid intensity and lineshape modifications due to the heating current. The BE scale has been calibrated with respect to the Fermi level E_F measured under the same experimental conditions. Different emission angles β were also used ranging from normal ($\beta = 0^\circ$, photon beam incidence of 70° with respect to surface plane) to grazing emission ($\beta = 80^\circ$).

We employed Fast-XPS [24], with energy resolution of 80 meV to monitor the Ir $4f_{7/2}$ SCL shifted components in real-time during oxygen adsorption at 300 K. The oxygen doses, expressed in Langmuir ($1L = 10^{-6}$ Torr s), are corrected for the ion gauge sensitivity factor. During the uptake, molecular oxygen was dosed by background exposure at different pressures (from 1×10^{-9} to 1×10^{-7} mbar). The acquisition time of each Ir $4f_{7/2}$ spectrum was of the order of 6 s.

All the photoemission spectra presented in this paper have been fitted using Doniach–Šunjić (DS) [25] functions, characterized by the Lorentzian width Γ and the Anderson singularity asymmetry parameter α that takes into account the electron–hole pair excitations and/or shake-up states, convoluted with a Gaussian (full-width at half-maximum G) which accounts for the instrumental resolution and phonon broadening/vibrational fine structure. In the fittings, performed using procedures written within the IGOR software, the background was assumed to be linear.

The Ir $4f_{7/2}$ core level spectrum corresponding to the clean surface, measured at $h\nu = 160$ eV and in normal emission conditions, is shown in figure 1(a). Two distinct components can be observed at 60.87 and 60.32 eV, which are assigned to photoemission from bulk and surface atoms, respectively.

Our analysis reveals that the best fit, obtained using two DS functions with different Γ ($\Gamma_{bulk} = 200$ meV and $\Gamma_{surface} = 320$ meV) and α ($\alpha_{bulk} = 0.15$ and $\alpha_{surface} = 0.22$), convoluted with Gaussians of different width ($G_{bulk} = 170$ meV and $G_{surface} = 90$ meV), is satisfactory, as indicated by the small modulation present in the residual. The deconvolution with just two components, shifted by 550 meV, is therefore sufficient to describe the lineshape of the Ir(111) $4f_{7/2}$ core-level spectrum at this photon energy. However, these lineshape parameters are slightly

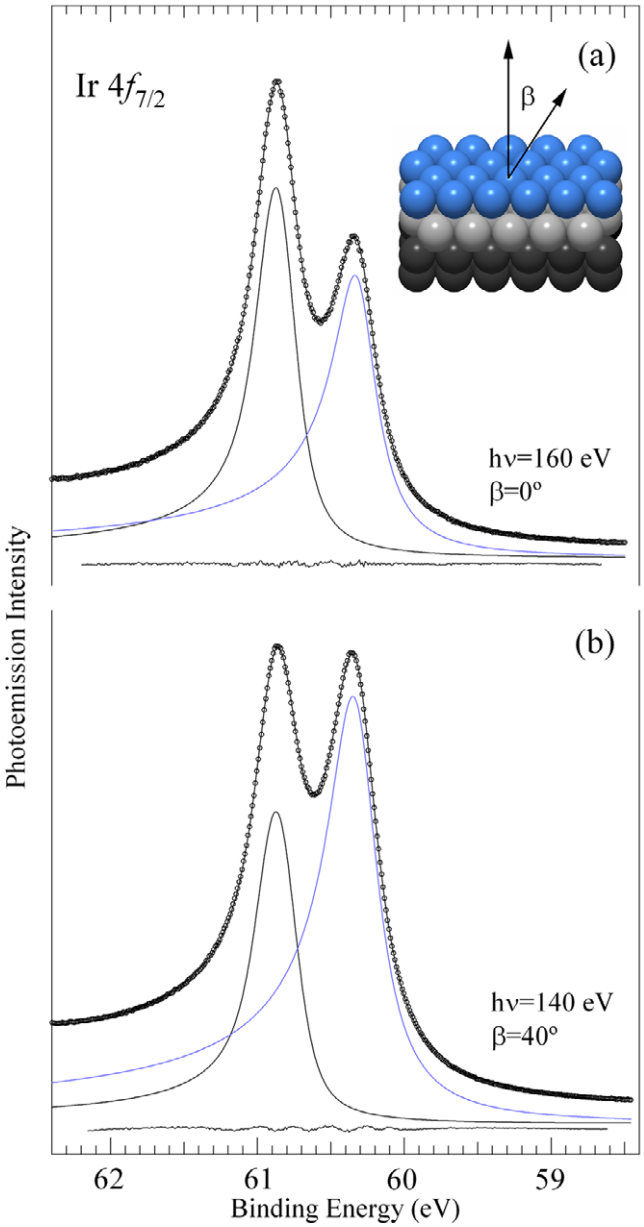

Figure 1. High-energy resolution Ir $4f_{7/2}$ core level spectra corresponding to the clean (1×1) Ir(111) surface measured at (a) $h\nu = 160\,\mathrm{K}$ and $\beta = 0^\circ$ (normal emission) and (b) $h\nu = 140\,\mathrm{K}$ and $\beta = 40^\circ$. Both spectra, measured at 80 K, can be fitted with two components corresponding to bulk (black) and first-layer atoms (blue) with a SCLS of $-550\,\mathrm{meV}$.

different from those found on the stepped Ir(210) [16], which were assumed to be the same for the three surface and bulk components ($\Gamma_B = 300\,\mathrm{meV}$, $\alpha_B = 0.12$ and $G_B = 150\,\mathrm{meV}$). What is more surprising in our results is that the Gaussian width of the bulk peak is larger than that of the surface, whereas the opposite behaviour is expected because of the higher vibrations at the surface giving additional phonon broadening.

In order to make an accurate determination of the SCLSs and of the lineshape parameters we adopted a procedure already used in other investigations [26]–[29]: we acquired spectra at different photon energies ($h\nu = 140$, 160, 180 and 200 eV) and emission angles ($\beta = 0°$, 20°, 40° and 60°) in order to change the surface sensitivity and the photoelectron diffraction conditions to modify the surface to bulk intensity ratio R.

From a simple inspection of the data it is possible to observe that, while for higher photon energies the low BE component is suppressed, for the spectrum at $\beta = 40°$ and $h\nu = 140$ eV (figure 1(b)), R is maximum. This effect cannot be explained only with inelastic mean free path arguments because the strong modulation of the lower BE peak is strongly affected by photoelectron diffraction effects.

The first analysis of the overall series of spectra was performed using two different DS functions, without constraints. Good convergence was achieved for the fits of the complete series, as confirmed by the structureless residual. We found a SCLS of -548 ± 15 meV, in very good agreement with recent theoretical calculations based on density functional theory, which give a value of -555 meV [30].

Although this result is quite similar to the previous findings (-0.50 ± 0.02 eV), it is not within the error bar. A possible reason for the discrepancy can be ascribed to the presence of contaminants in the previous experiments (hydrogen, water, CO), which are known to shift the surface component of a metal with a d-band more than half-filled towards higher BE. More recently, SCLS measurements of the $4f_{7/2}$ core level of clean Ir(210) have evidenced that all surface features are shifted towards lower BE. In particular the component originated by second-layer atoms, with a nominal coordination of 9, as for the Ir(111) surface atoms, presents a SCLS of -529 meV, which is closer to our findings. Nevertheless we have to keep in mind that slight modifications of the inter-atomic distances, due to first-to-second layer relaxation of the stepped surface, are known to induce modifications in the core level shift.

The behaviour of the lineshape parameters deserves further considerations. A summary of the results is reported in figure 2. A correlation between Lorentzian and Gaussian widths of the bulk and surface components is evident: larger values of Γ correspond to minima of G_B.

In order to rationalize the data analysis procedure, we mapped the evolution of the chi-square χ^2 as a function of each parameter, following the procedure proposed in [8, 29]. The two-dimensional χ^2 contour plot (Γ_{bulk} versus G_{bulk}), reported in figure 3(a), shows a pronounced and localized minimum, contrary to what observed in figure 3(b) for the surface component. Moreover, the fitting results revealed an additional feature, which is present in the whole data analysis: a high cross-correlation is present between Γ_B and G_B, Γ_B and I_B, G_B and I_B, while this does occur to a lesser extent for the surface peak. We interpret this effect as due to the higher sensitivity of the bulk peak to small variations of the DS parameters.

The best lineshape parameters we obtained are: $\Gamma_B = 200$ meV, $\alpha_B = 0.135$, $G_B = 170$ meV and $\Gamma_S = 310$ meV, $\alpha_S = 0.225$ and $G_S = 70$ meV.

Possible reasons accounting for the larger Gaussian width of the bulk, compared with that of the surface, are given in the following paragraph.

The first relates to the possible limit of applicability of the DS function for fitting the Ir 4f core level. Contrary to Pt, where the Fermi level lies in a strongly varying density of states, the Fermi level of Ir lies in a region where the density of states is quite flat, which is the assumption implicit in the DS equation. Therefore the larger Gaussian width of the bulk component cannot be attributed to a wrong representation of the Ir 4f with the DS lineshape.

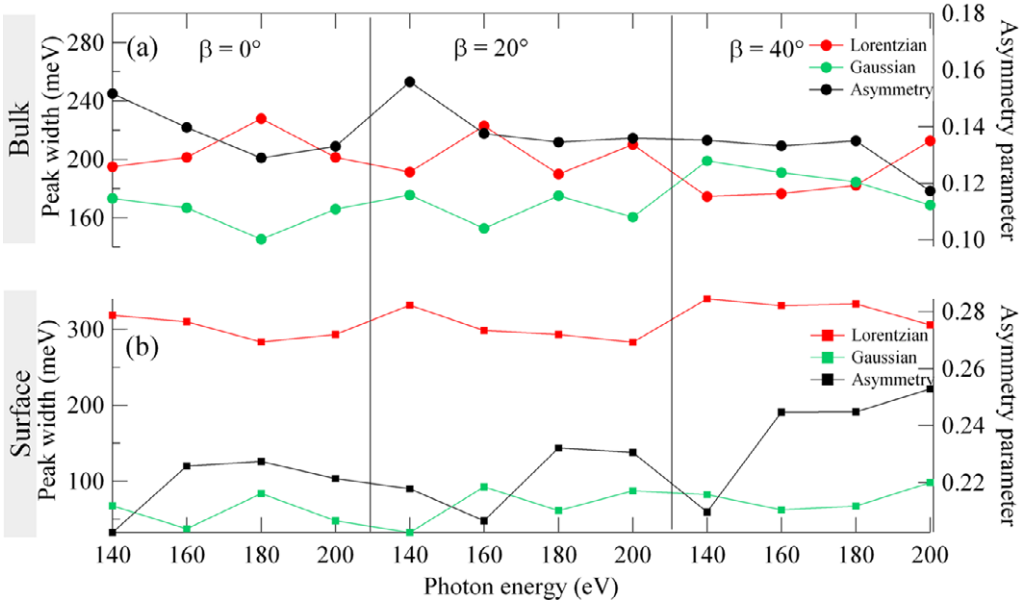

Figure 2. Lorentzian, Gaussian (left axes) and asymmetry parameters (right axes) of (a) bulk and (b) surface components, as obtained by fitting the Ir $4f_{7/2}$ core level spectra measured at $h\nu = 140$, 160, 180 and 200 eV and emission angles $\beta = 0^\circ$, 20° and 40°.

The most plausible reason for this unexpected finding is the presence of subsurface layer components in the close vicinity of the bulk peak, which are not included in our fitting analysis: the slightly different BE of the atoms in the layers below the topmost surface results in inhomogeneous broadening of the bulk peak. The same behaviour was indeed found also for the Ta(100) surface [31]. Despite the close-packed geometry of fcc(111) surfaces, where the second layer atomic coordination is the same as that of the bulk, experimental and theoretical studies have reported SCLSs also for the second-layer atoms. Other systems where the second-layer SCLS has been revealed are Ta(110) [8], W(110) [11], W(111) [12], Ru(1010) [27], Ru(0001) [28], Rh(111) [29], Rh(110) and Rh(100) [32].

Another interesting finding of our SCLS analysis is the different Anderson singularity index α of bulk and surface components, reported in figure 3, which can be described in terms of the orbital character of the conduction band charge. Theoretical studies have shown that final state effects at clean transition metal surfaces are dominated by intra-atomic d-electron screening [33] and are manifested in the spectra as a high-BE power-law tail described by the singularity index α. The α parameter found in the data analysis indicates that the conduction-electron screening is larger for the first layer ($\alpha = 0.225$) than for the bulk atoms ($\alpha = 0.135$). This behaviour has already been experimentally observed for other 5d transition metal surfaces. For example a singularity index α of 0.10 and 0.205 [31] was found for the bulk and surface components of Ta(100), respectively.

In figure 3 we report also the Lorentzian width Γ. The larger Γ of the surface component ($\Gamma_S = 310$ meV) compared with the bulk ($\Gamma_B = 200$ meV) is an indication that the increased localization of the more atomic-like d-electron charge density at the surface enhances the intra-atomic Auger core-valence probability. Similar trends were found also for Ta(100)

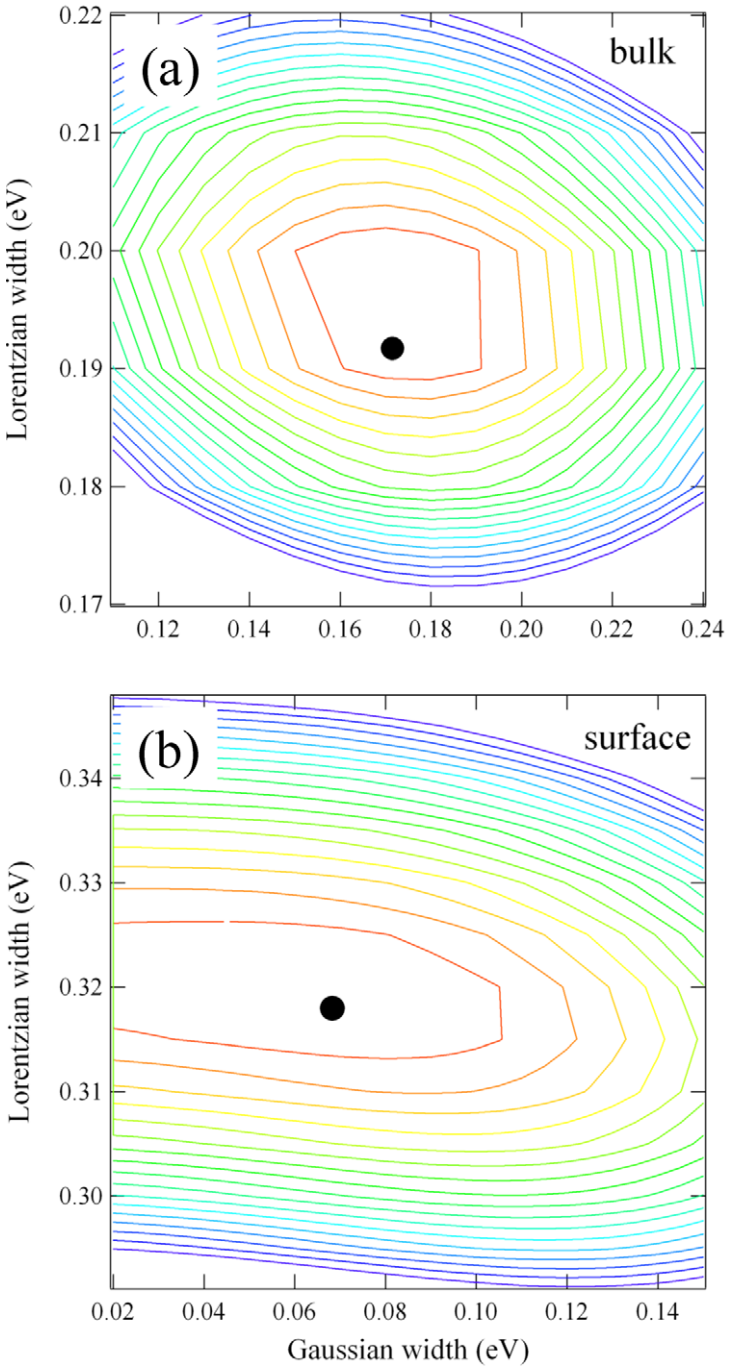

Figure 3. Two-dimensional χ^2 contour plots referred to the fit of the Ir $4f_{7/2}$ core level spectrum measured at $h\nu = 140$ and $\beta = 0^\circ$. (a) The Lorentzian width versus Gaussian width for bulk component shows a pronounced and localized minimum. (b) Contrary to the (a) plot, the Lorentzian width of the surface component does not strongly depend on the Gaussian width of the surface component.

($\Gamma_S = 70$ meV and $\Gamma_B = 37$ meV) [31], Rh(110) ($\Gamma_S = 245$ meV and $\Gamma_B = 165$ meV) and Rh(100) ($\Gamma_S = 270$ meV and $\Gamma_B = 165$ meV) surfaces [32].

In order to univocally determine the relevance of the phonon contribution to the Gaussian width of bulk and surface components the temperature dependence of the Ir $4f_{7/2}$ lineshape was measured in the temperature range between 90 and 890 K. The spectra, collected at $h\nu = 180$ eV and normal emission, are shown in figure 4. From the inspection of the raw data, one clearly observes that the two peaks broaden as the temperature increases. Within the temperature range investigated, the main contribution to the linewidth comes from the phonon distribution. A quantitative assessment of the temperature dependence of the lineshape was carried out with a least-squares analysis. Each spectrum was analysed by letting the BE of bulk and surface components and the Gaussian width be free parameters, the latter accounting for the phonon contribution and the temperature-independent instrumental resolution, while Γ and α were fixed to their low temperature values. This is an adequate choice, because in a first approximation the core-hole lifetime and the electron–hole pair excitation probability do not depend on the temperature.

Figure 5(a) shows the square of the Gaussian width as a function of temperature of the bulk and surface peaks: both curves show almost linear behaviour. These results confirm the larger Gaussian contribution of the bulk component at low temperature, while most notable is the difference of the slope of the surface and bulk curves. In parallel with broadening, both components shift towards lower BE with increasing temperature, as shown in figure 5(b), the bulk-peak by 31 meV, the surface-peak by 17 meV, between 80 and 780 K. Therefore the SCLS decreases by 14 meV.

We analysed the behaviour of the Gaussian width using the Hedin and Rosengren model [33] for the phonon broadening, based on the Debye model, where the squared G^2 is given by,

$$G_T^2 = G_{\mathrm{res}}^2 + G_{\mathrm{inh}}^2 + G_{\mathrm{p}}^2(0)\left[1 + 8\left(\frac{T}{\theta_{\mathrm{D}}}\right)^4 \int_0^{\theta_{\mathrm{D}}/T} \mathrm{d}x \frac{x^3}{\mathrm{e}^x - 1}\right]. \tag{1}$$

Here, G_{res} and G_{inh} are the widths of the instrumental resolution and inhomogeneous broadening, respectively, $G_{\mathrm{p}}(0)$ is the phonon broadening at $T = 0$ K and Θ_{D} is the Debye temperature. This equation can be applied for $T/\Theta_{\mathrm{D}} > 0.8$. Using a least-squares analysis we obtained $\Theta_{\mathrm{D}}(\mathrm{bulk}) = 298 \pm 8$ K and $\Theta_{\mathrm{D}}(\mathrm{surf}) = 181 \pm 3$ K, which are in very good agreement with previously determined values obtained using LEED, i.e. 315 ± 22 and 170 ± 12 K for bulk and surface Debye temperature, respectively [18].

The BE changes of bulk and surface components could be related to a change in the valence-band density of states as the lattice expands, even though final-state effects (changes in relaxation energy as the screening length changes) are expected to contribute.

The different behaviour of the surface and bulk thermal shifts is in strict contrast to the results obtained on alkali metals [34] where, despite the large thermal shifts, no difference was observed between the thermal shift of the bulk and surface core level components.

Using the Friedel model combined with a linear combination of atomic orbitals, Riffe *et al* [9] calculated a shift of -0.058 meV K^{-1} for the core level of bulk Ir. Our results seem to validate this simple model. First of all the experimental shifts are negative, as expected when the d-band is more than half-filled, as for Ir. Moreover, we find a thermal shift of -0.045 and -0.024 meV K^{-1}, for the bulk and surface components, respectively. While the thermal shift of the Ir $4f_{7/2}$ of the bulk is in good agreement with the model, the difference found for the

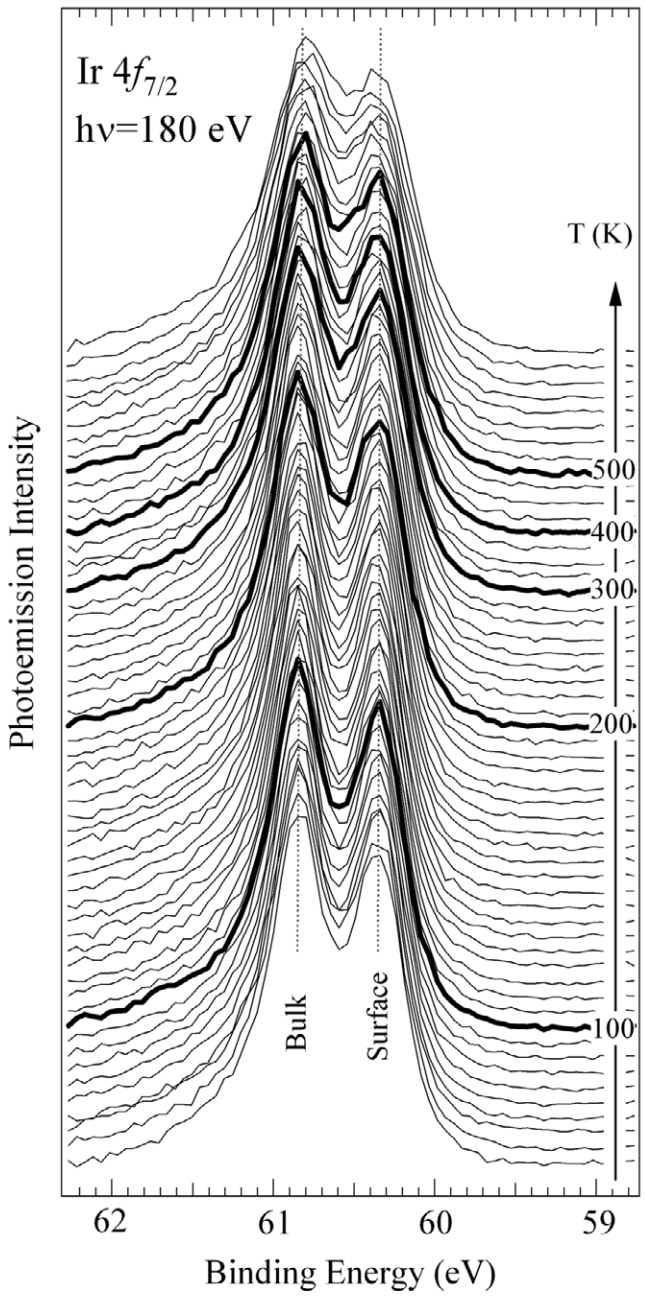

Figure 4. Temperature evolution of the Ir $4f_{7/2}$ core level spectra measured in the range 80–780 K and $h\nu = 180$ eV. Each spectrum was acquired in 6 s. The two lines mark the position of the surface and bulk components.

temperature behaviour of the surface peak can be ascribed to the different bulk and first-to-second layer expansion. In the case of Be(0001) for example, where the first three topmost layers can be distinguished in the Be 1s core level spectra, the SCLS of the first- and second-layer atoms decreases, while that of the third layer increases at higher temperature [35]: the comparison of the experimentally determined SCLS with density functional theory calculations was used to find the temperature-dependent interlayer distances. Another example is the Ta(100)

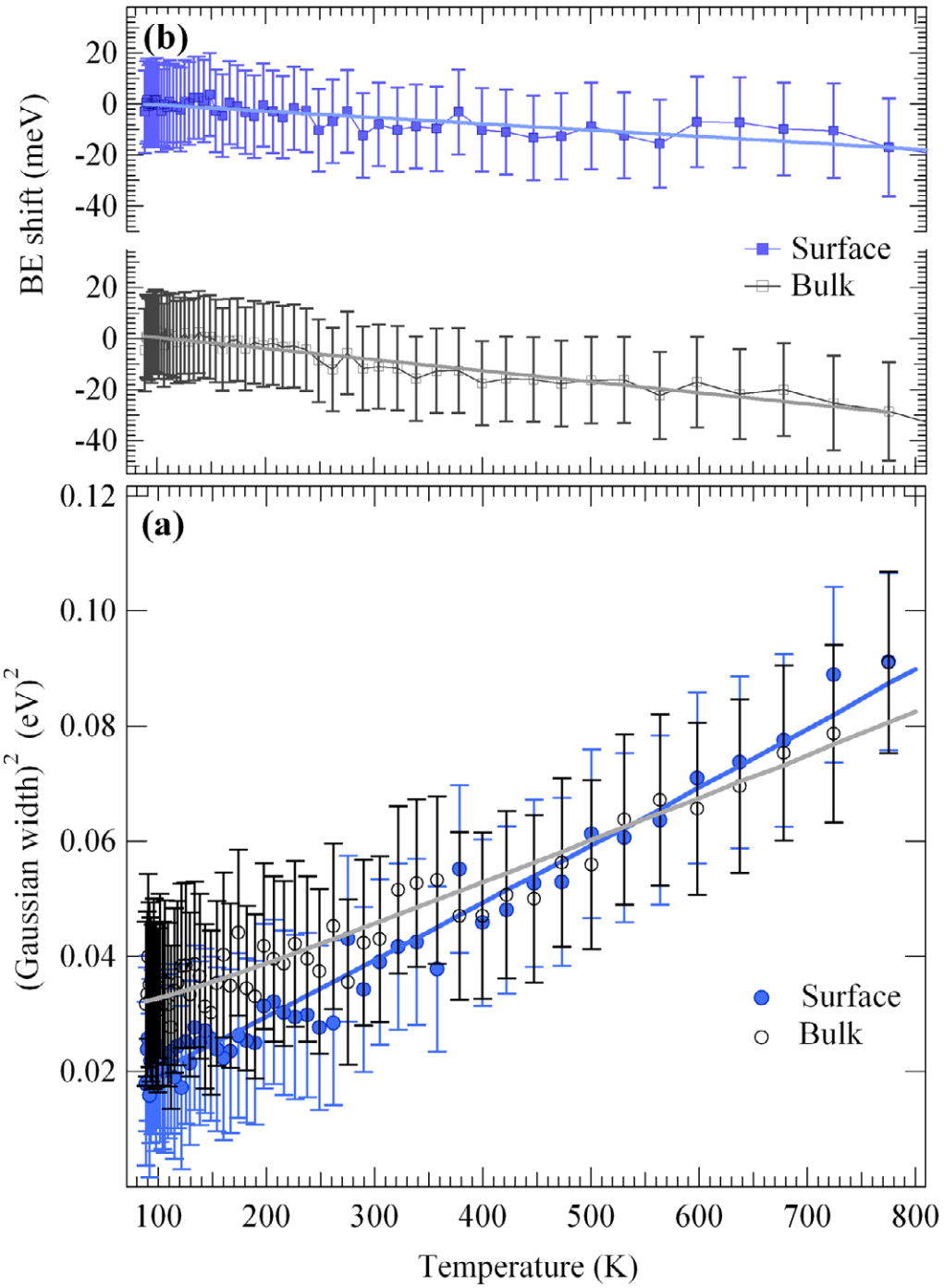

Figure 5. (a) Square of the total Gaussian width versus temperature for Ir $4f_{7/2}$ bulk (black) and surface (blue) components. Note the different slope of the surface line. (b) BE shifts for the bulk (black) and surface (blue) components of Ir $4f_{7/2}$ core level spectra measured in the range 80–780 K and $h\nu = 180$ eV. The solid lines are linear least-squares fits through the experimental data points.

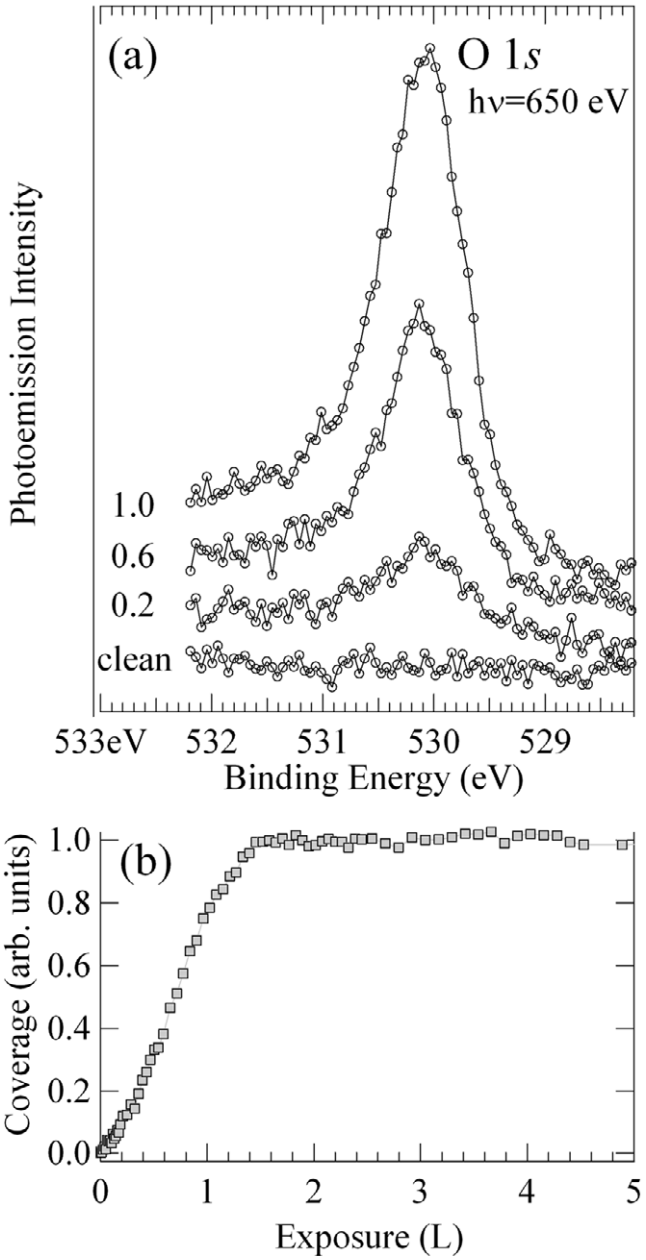

Figure 6. (a) O 1s selected spectra measured during oxygen uptake at $T = 80\,\mathrm{K}$. Oxygen pressure ranges from 1×10^{-9} to 1×10^{-7} mbar. $h\nu = 650\,\mathrm{eV}$. The oxygen coverage corresponding to each spectrum, normalized to the saturation coverage, is indicated on the left. (b) Oxygen uptake curve calculated by fitting the O 1s spectra. Note that saturation is reached already at about 1.5 L.

surface, where the thermal shift of the bulk Ta 4f component is ~ 2.4 times larger than that of the surface peak [9].

The final step of our investigation was the study of the changes induced on the Ir $4f_{7/2}$ SCLS by oxygen adsorption.

Previous LEED studies of O_2 dissociative adsorption on Ir(111) have evidenced the presence of a pattern with (2×2) periodicity [18]. XPS and HREELS (high resolution electron energy loss spectroscopy) data [21, 22] suggested that the saturation coverage is 0.5 ML. This corresponds to a $p(2 \times 1)$ structure with three domains rotated by 120° from each other, giving the same LEED pattern as a single $p(2 \times 2)$ domain, and with a single oxygen adsorption site, as suggested by the observation at the saturation coverage of one loss peak in HREELS at 550 cm^{-1} [19]. A LEED I–V investigation [18], although not decisive for the determination of the saturation coverage, concluded that the preferred adsorption site is threefold. Theoretical calculations [36, 37] reported that the dissociation is nearly spontaneous, with a very small activation energy of 0.06 eV $molecule^{-1}$. Similarly to oxygen adsorption on other transition metal surfaces, as the coverage increases from 0.25 to 1.0 ML, the BE decreases substantially, because of the repulsive interaction between the adsorbed atoms [38].

Figure 6(a) shows a selection of the O 1s spectra collected during oxygen uptake at 80 K. The sequence of spectra, measured at $h\nu = 650$ eV, can be fitted using a single peak up to the saturation exposure of 1.5L. As shown in figure 6(b), the intensity of the O 1s peak increases with increasing oxygen coverage. The shift of the O 1s towards lower BE is rather small, less than 70 meV, and cannot be assigned to a change of the oxygen adsorption site. In an initial-state picture the O 1s BE variation can be understood by taking into consideration that, as the oxygen coverage increases, the distance between negatively charged O atoms decreases and a repulsive interaction builds up. This produces changes in O–Ir bond length which results in small variations of the BE. Therefore our results suggest that oxygen preserves the same adsorption site in agreement with previous experimental [19] and density functional theory [23, 36] investigations.

In order to monitor the rearrangements in the adsorbed phase at increasing coverage, we have measured the Ir $4f_{7/2}$ SCLSs induced by the oxygen atoms. These measurements offer the unique possibility of identifying the changes in the local environment of the substrate atoms, like the number of O atoms bound to each Ir surface atom.

The real-time SCLS method [23] has been applied to probe the evolution of the Ir $4f_{7/2}$ core level during oxygen adsorption. Figure 7 shows the series of Ir $4f_{7/2}$ spectra measured in the same experimental conditions used for the O 1s experiments. The spectrum of the clean surface consists of two well resolved Ir_{bulk} and Ir_0 peaks representing the emission from the bulk and the surface atoms, respectively, as explained above. Oxygen adsorption at low coverage leads to the appearance of a new component Ir_1 which grows between the surface and the bulk peaks, while the intensity of the original Ir_0 surface peak decreases. At higher coverage, Ir_0 further decreases and a third surface component Ir_2 grows at BE larger than the bulk peak.

The deconvolution of the Ir $4f_{7/2}$ spectra has been performed using for the extra components Ir_1 and Ir_2, the same lineshape parameters of the clean surface component Ir_0. Moreover, in the fitting procedure the BE positions of Ir_1 and Ir_2 were allowed to vary in a limited energy range, as explained below. A first attempt was performed leaving the BEs of all the peaks free, in order to detect acceptable ranges of variation. This fitting procedure achieved convergence only for some spectra; however, it allowed to determine the proper BE intervals for bulk, Ir_0, Ir_1 and Ir_2. The results of the fits of the whole series of spectra measured at different oxygen coverage, reported in figure 8, have been obtained by setting stronger constraints on the BE intervals as a function of the relative intensity of the peaks, the BE being more precisely identified when the intensity of a component is high. While the BE position of the bulk peak remains constant, as expected, a small shift of about 50 meV towards higher BE is experienced

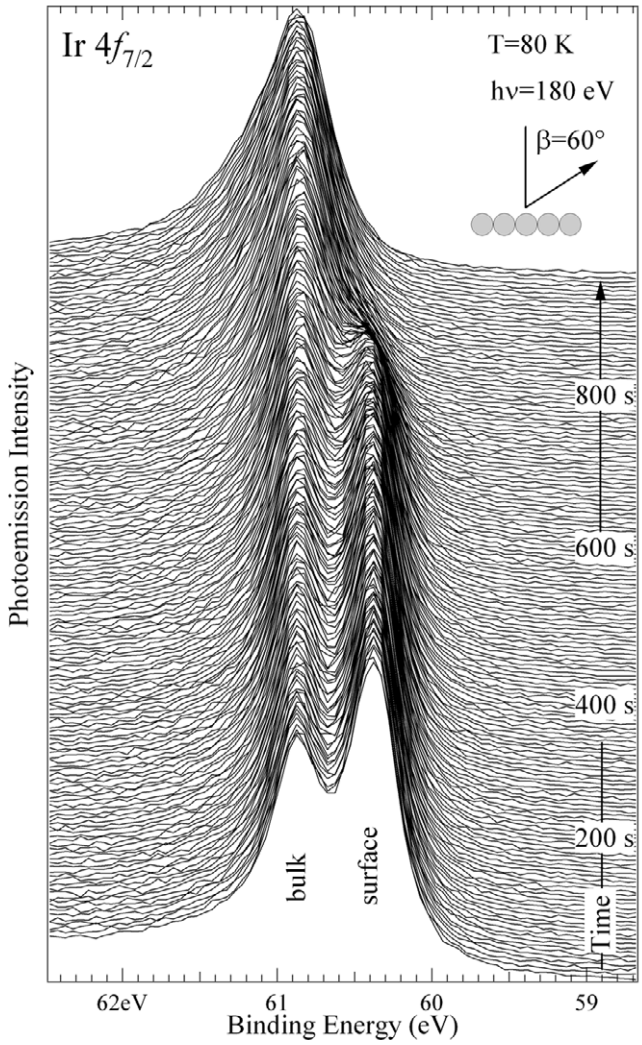

Figure 7. Evolution of the Ir $4f_{7/2}$ core-level spectra during oxygen adsorption on Ir(111) at $T = 80$ K. Oxygen pressure ranges from 1×10^{-9} to 1×10^{-7} mbar, $h\nu = 180$ eV.

by Ir_0 at increasing oxygen coverage. The Ir_1 component was found to be at -200 ± 20 meV with respect to the bulk peak, while the SCLS of Ir_2 is $+230 \pm 30$ meV. The larger error bar of the SCLS of Ir_2 is due to the low intensity of this component and the close vicinity to the bulk peak that makes the deconvolution more difficult. From a close comparison with the behaviour of the SCLSs induced by dissociative oxygen adsorption on other substrates [7, 28, 39, 40] we assign the Ir_1 and Ir_2 components to first-layer Ir atoms single and double-bonded with oxygen atoms.

An important piece of information provided by these experiments concerns the oxygen induced changes in the local electronic structure of the surface atoms, obtained by the measurement of the BE difference ΔE of Ir_1 and Ir_2 with respect to the clean component Ir_0. Indeed, since $\Delta E_1 = +350$ meV and $\Delta E_2 = +780$ meV, it turns out that $\Delta E_1 \approx 2 \times \Delta E_2$. This demonstrates the validity of the additivity rule of the oxygen-induced energy shift on the

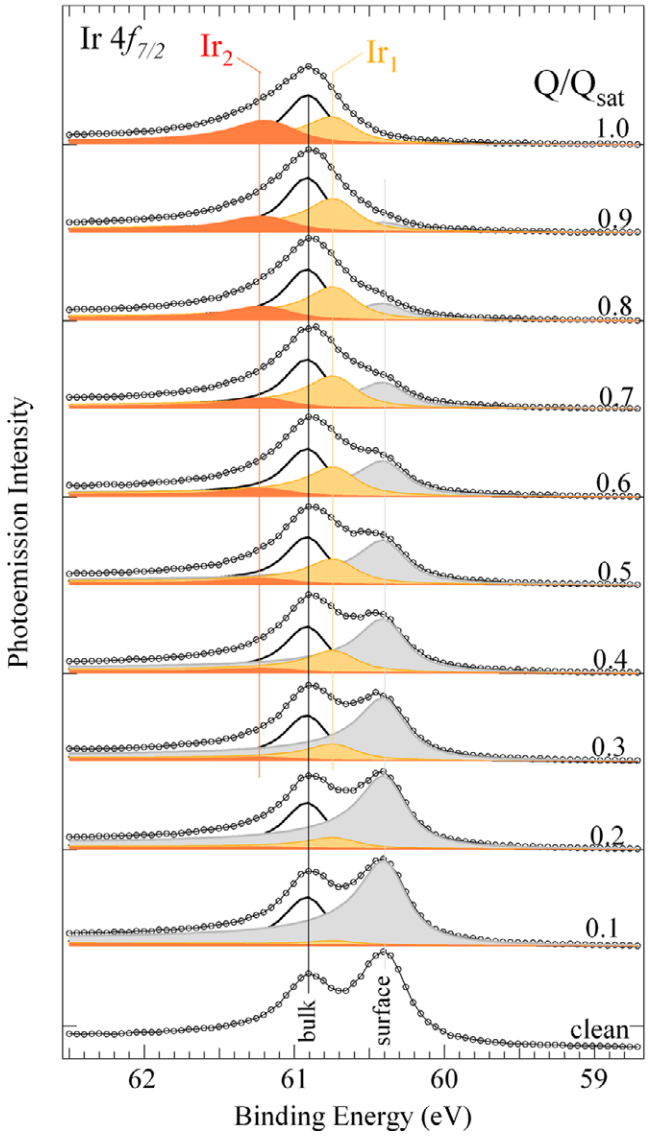

Figure 8. Evolution of the bulk and surface components of selected Ir $4f_{7/2}$ core-level spectra reported in figure 7. The Q/Q_{sat} oxygen coverage is reported on the right. Different colours correspond to surface Ir atoms in different local configurations. The grey component Ir_0 originates from the clean surface Ir atoms, while Ir_1 and Ir_2 peaks originate from surface Ir atoms which bind to one and two oxygen atoms, respectively.

Ir surface, a property that was already found on other adsorbate [38]–[41] and coadsorbate systems [42]. The almost linear dependence of ΔE on the number of O atoms bound to each Ir atom, reveals that the type of bonding of O remains the same in all the overlayers studied.

The oxygen-induced Ir 4f shift towards higher BE with increasing oxygen coverage can be qualitatively understood as due to charge transfer from the surface to the adsorbate. A complete understanding of this shift cannot be achieved only on these grounds because effects other than simple charge transfer play a crucial role in determining the SCLS.

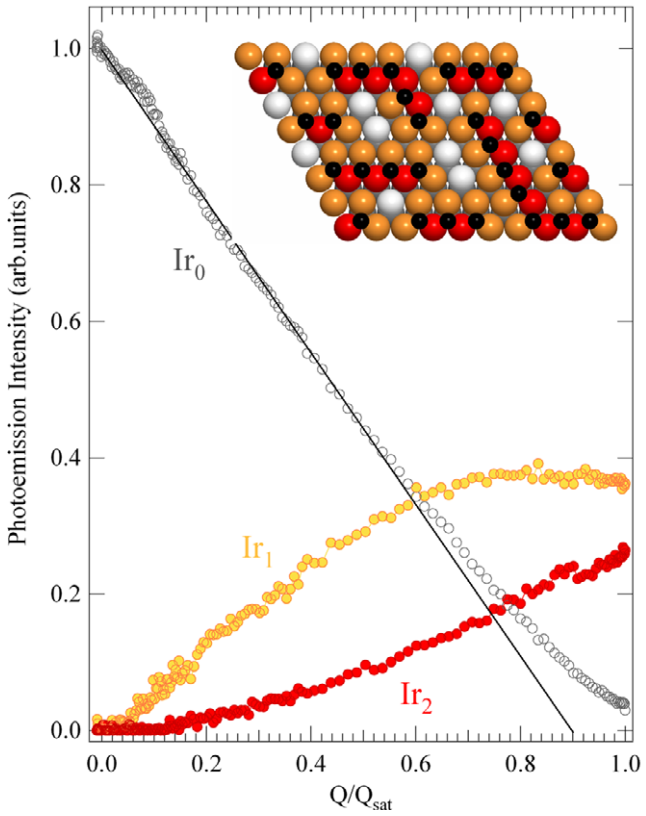

Figure 9. Intensity of the Ir $4f_{7/2}$ surface core level components as functions of oxygen coverage at 80 K. The first-layer features are associated with the non-equivalent surface iridium species: Ir_0 represents the clean surface Ir atoms (grey); Ir_1 represents Ir atoms with a single bond with oxygen (orange), and Ir_2 (red), Ir atoms with a double bond with oxygen. Tentative model structure of the oxygen layer formed at saturation. Note the intercept of the Ir_0 component linear fit at $Q/Q_{sat} \sim 0.9$.

A strong correlation between ΔE and the calculated valence d-band shift projected onto the surface atoms was found for many oxygen–transition metal systems. The oxygen adsorption typically induces a broadening of the d-band, along with a lowering of the density of states in the Fermi level region. This results in a d-band centre shift towards higher BEs with increasing oxygen coverage, which is reflected in the measured adsorbate-induced SCLSs. This effect applies also to the case of Ir.

Figure 9 displays the behaviour of the integrated intensities of Ir_0, Ir_1 and Ir_2 peaks as a function of the oxygen coverage. We show in the following paragraph that these functions contain detailed information on the kinetics of site occupation during chemisorption.

The Ir_0 surface component intensity is proportional to the number of first-layer clean Ir atoms, i.e. atoms that are not chemically bound to oxygen atoms [23]. At the beginning of the uptake, when the sample is clean, all Ir surface atoms are zero-coordinated to oxygen atoms. We normalize all intensities to this value.

In the early stage of oxygen adsorption the number of Ir_1 atoms linearly increases with oxygen uptake at the expense of the Ir_0 atoms. The Ir_2 component appears and grows later,

becoming appreciable only when the oxygen coverage Q is about 20% of the saturation coverage Q_{max} and reaches the maximum value just at saturation. At this coverage, the intensity of Ir_0 component remains significant, while the Ir_1 component has an intensity which is about 25% larger than the Ir_2 component.

The quantitative description of the adsorption phenomenon can be achieved through the observation of the clean surface signal, the only reliable indicator, since Ir_1 and Ir_2 intensities may well be affected by photoelectron diffraction effects. Therefore our analysis focuses on the Ir_0 curve, in particular on the slope of the initial linear behaviour. The decreasing intensity is a clear indication of adsorption: for each new oxygen atom adsorbed in threefold configuration, the intensity contribution of three surface Ir atoms should move from Ir_0 to Ir_1.

From this observation we calibrated the surface coverage in a straightforward way by simply assuming that the intercept of the linear fit of the Ir_0 curve is $1/3$, because of the already known adsorption in threefold configuration. This procedure was already applied on other adsorbate systems [23]. We found an oxygen saturation coverage of 0.38 ± 0.04 ML, a result that reconciles previous experimental and theoretical observations.

Indeed recently Stampfl *et al* [23] reported that the (2×2)-O structure with 0.25 ML coverage is the only chemisorbed phase that is predicted to be stable on the surface, and only for a very narrow range of the oxygen chemical potential, which can be achieved in UHV conditions. These results suggest that the saturation coverage of 0.5 ML, reported by the experiments, may only be metastable with respect to bulk oxide formation. Our results indicate that the $p(2 \times 1)$ structure cannot be experimentally obtained without a certain degree of surface disorder, like oxygen vacancies in the lattice, as reported in the structural model reported in figure 9. These findings underline the importance of considering the problem of pressure gap encountered in usual surface science studies, and its consequences on surface morphology. On Ir(111), when using oxygen exposures in the 10^{-7} mbar range even for prolonged time, the coverage at saturation remains always below 0.5 ML: the increase of O_2 pressure and substrate temperature are therefore the key ingredients to produce a stable high coverage oxygen structure, which represents an intermediate step towards the subsurface penetration and the formation of Ir surface oxide, as predicted by theory [23]. Our results therefore confirm that the room temperature instability of a long-range oxygen ordered structure at 0.5ML is not due to reducing agents (CO, H_2, etc) as supposed, but originates from the intrinsic properties of the O–Ir interface. The recent development of high pressure XPS technique with synchrotron radiation can be the base for testing the results with recent ab initio calculations about the stability of oxide species formed on Ir at higher temperature and pressure [23].

In summary, we have shown that the extreme sensitivity of core-level spectroscopy to the local electronic environment of surface atoms can be exploited to monitor the evolution of a wide range of phenomena taking place on solid surfaces. In particular the direct *in situ* and real-time measurement of core-level changes have proven decisive for an in-depth understanding of different properties of clean and oxygen covered Ir(111). The accurate determination of Ir $4f_{7/2}$ core level BE and lineshape parameters allowed us to probe the electronic structure of first-layer Ir atoms. The larger Gaussian width of the bulk component compared with the surface, is explained as due to the presence of unresolved subsurface components (second and deeper layers). The temperature evolution of the Gaussian widths was used to determine surface and bulk Debye temperature, which are in good agreement with previous electron diffraction measurements. Finally the oxygen adsorption process was investigated by monitoring in situ the changes in the Ir $4f_{7/2}$ core level spectra. The unambiguous identification of Ir surface

atoms differently coordinated with oxygen and the behaviour of the corresponding intensities indicate that the oxygen coverage achieved in UHV conditions is below 0.5 ML, as predicted by theoretical calculations.

Acknowledgments

AB thanks the Sincrotrone Trieste SCpA for providing the access to the Elettra Laboratory and for the support received during the beamtime allocated at the SuperESCA beamline for the 'Laboratorio di Fisica della Materia B' of the Trieste University. P Lacovig and P Vilmercati are also acknowledged for their help during the measurements. AB acknowledges precious technical support from Angst-Pfister.

References

[1] van den Broek A C M, van Grondelle J and van Santen R A 1999 *J. Catal.* **185** 297
[2] Johnson D F and Weinberg W H 1993 *Science* **261** 76
[3] N'Diaye A T, Bleikamp S, Feibelman P J and Michely T 2006 *Phys. Rev. Lett.* **97** 215501
[4] Egelhoff W F Jr 1986 *Surf. Sci. Rep.* **6** 253
[5] Spanjaard D, Guillot C, Desjonqueres M C, Treglia G and Lecante J 1985 *Surf. Sci. Rep.* **5** 1
[6] Mårtensson N and Nilsson A 1994 *High Resolution Core-Level Photoelectron Spectroscopy of Surfaces and Adsorbates (Springer Series in Surface Science* vol 35) (Berlin: Springer) p 65
[7] Baraldi A 2008 *J. Phys.: Condens. Matter* **20** 093001
[8] Riffe D M and Wertheim G K 1993 *Phys. Rev.* B **47** 6672
[9] Riffe D M, Hale W, Kim B and Erskine J L 1996 *Phys. Rev.* B **54** 17118
[10] Riffe D M, Wertheim G K and Citrin P H 1989 *Phys. Rev. Lett.* **63** 1976
[11] Riffe D M, Wertheim G K, Citrin P H and Buchanan D N E 1990 *Phys. Scr.* **41** 1009
[12] Wertheim G K and Citrin P H 1988 *Phys. Rev.* B **38** 7820
[13] Puglia C, Nilsson A, Hernnäs B, Karis O, Bennich P and Mårtensson N 1995 *Surf. Sci.* **342** 119
[14] Baraldi A *et al* 2007 *J. Chem. Phys.* **127** 164702
[15] van der Veen J F, Himpsel F J and Eastman D E 1980 *Phys. Rev. Lett.* **44** 189
[16] Gladys M J, Ermanoski I, Jackson G, Quinton J S, Roweb J E and Madey T E 2004 *J. Electron Spectrosc. Relat. Phenom.* **135** 105
[17] Johansson B and Mårtensson N 1983 *Helv. Phys. Acta* **56** 405
[18] Chan C M, Williams B D and Weinberg W H 1979 *Surf. Sci.* **82** L577
[19] Davis J E, Nolan P D, Karseboom S G and Mullins C B 1997 *J. Chem. Phys.* **107** 943
[20] Chan C M and Weinberg W H 1979 *J. Chem. Phys.* **71** 2788
[21] Zhdan P A, Boreskov G K, Boronin A I, Egelhoff W F and Weinberg W H 1976 *Surf. Sci.* **61** 25
[22] Marinova T S and Kostov K L 1987 *Surf. Sci.* **185** 203
[23] Stampfl C, Soon A, Piccinin S, Shi H and Zhang H 2008 *J. Phys.: Condens. Matter* **20** 184021
[24] Baraldi A, Comelli G, Lizzit S, Kiskinova M and Paolucci G 2003 *Surf. Sci. Rep.* **49** 169
[25] Doniach S and Šunjiċ M 1970 *J. Phys. C: Solid State Phys.* **3** 185
[26] Lizzit S, Pohl K, Baraldi A, Comelli G, Fritzsche V, Plummer E W, Stumpf R and Hofmann P 1998 *Phys. Rev. Lett.* **81** 3271
[27] Baraldi A, Lizzit S, Comelli G, Goldoni A, Hofmann P and Paolucci G 2000 *Phys. Rev.* B **61** 4534
[28] Lizzit S *et al* 2001 *Phys. Rev.* B **63** 205419
[29] Baraldi A, Lizzit S, Novello A, Comelli G and Rosei R 2003 *Phys. Rev.* B **67** 205404
[30] Lacovig P, Pozzo M, Alfè D, Vilmercati P, Baraldi A and Lizzit S submitted
[31] Riffe D M, Hale W, Kim B and Erskine J L 1995 *Phys. Rev.* B **51** 11012

[32] Zacchigna M, Astaldi C, Prince K C, Sastry M, Comicioli C, Evans M and Rosei R 1996 *Phys. Rev.* B **54** 7713
[33] Hedin L and Rosengren A 1977 *J. Phys. F: Met. Phys.* **7** 1339
[34] Riffe D M, Wertheim G K, Buchanan D N E and Citrin P H 1992 *Phys. Rev.* B **45** 6216
[35] Baraldi A, Lizzit S, Pohl K, Hofmann P and de Gironcoli S 2003 *Europhys. Lett.* **64** 364
[36] Xu Y and Mavrikakis M 2002 *J. Chem. Phys.* **116** 10846
[37] Krekelberg W P, Greeley J and Mavrikakis M 2004 *J. Phys. Chem.* B **108** 108
[38] Baraldi A, Lizzit S, Comelli G, Kiskinova M, Rosei R, Honkala K and Nørskov J K 2004 *Phys. Rev. Lett.* **93** 046101
[39] Vesselli E, Baraldi A, Bondino F, Comelli G, Peressi M and Rosei R 2004 *Phys. Rev.* B **70** 115404
[40] Ganduglia-Pirovano M V, Scheffler M, Baraldi A, Lizzit S, Comelli G, Paolucci G and Rosei R 2001 *Phys. Rev.* B **63** 205415
[41] Bianchettin L, Baraldi A, de Gironcoli S, Lizzit S, Petaccia L, Vesselli E, Comelli G and Rosei R 2006 *Phys. Rev.* B **74** 45430
[42] Lizzit S, Zhang Y, Kostov K L, Petaccia L, Baraldi A, Larciprete R, Menzel D and Reuter K 2009 *J. Phys.: Condens. Matter* **21** 134009